Microscopy Research and Technique

Super-resolution imaging with stochastic single molecule localization: concepts, technical developments and biological applications

Journal:	*Microscopy Research and Technique*
Manuscript ID:	MRT-13-338.R1
Wiley - Manuscript type:	Review Article
Date Submitted by the Author:	n/a
Complete List of Authors:	Oddone, Anna; ICFO-Institute of Photonic Sciences, Vilanova, Ione; ICFO-Institute of Photonic Sciences, Tam, Johnny; ICFO-Institute of Photonic Sciences, Lakadamyali, Melike; ICFO-Institute of Photonic Sciences,
Keywords:	super-resolution, STORM, PALM

Super-resolution imaging with stochastic single molecule localization: concepts, technical developments, and biological applications

Anna Oddone[1], Ione Verdeny Vilanova[1], Johnny Tam[1], Melike Lakadamyali[1*]

[1]ICFO - Institut de Ciències Fotòniques

Mediterranean Technology Park

08860, Castelldefels (Barcelona), Spain

[*] Correspondence should be sent to: melike.lakadamyali@icfo.es

Abstract

Light microscopy has undergone a revolution with the advent of super-resolution microscopy methods that can surpass the diffraction limit. These methods have generated much enthusiasm, in particular with regards to the new possibilities they offer for biological imaging. The recent years have seen a great advancement both in terms of new technological developments and exciting biological applications. Here, we review some of the important milestones in the field and highlight some recent biological applications.

Introduction

Fluorescence microscopy is a powerful tool for biology, as it enables the visualization of dynamic biological phenomena in multiple colors, in three dimensions, and with very high molecular specificity. Until recently, however, a main drawback of fluorescence microscopy (and of all other light microscopy techniques) has been the limited spatial resolution achievable with light due to diffraction. The resolving power of an optical microscope can be approximated by $\lambda/(2NA)$ in the lateral (x-y) directions and $(2\lambda n)/NA^2$ in the axial (z) direction, where NA is the numerical aperture of the microscope objective, λ the wavelength of light, and n the refractive index of the medium. When imaging with visible light through high-NA objectives, the resolution of conventional light microscopes is thus limited to ~200 nm and ~500 nm in the lateral and axial directions, respectively. This limitation is highly problematic in biology because many biological structures are below the diffraction limit (e.g. protein complexes, DNA, cytoskeletal filaments, vesicles, and viruses). Over the past several years, this limitation has been overcome with the development of new techniques that can achieve resolutions more than one order of magnitude beyond that imposed by the diffraction limit. These methods include stimulated emission depletion microscopy (STED) (Klar and Hell, 1999; Klar and others, 2000), saturated structured illumination microscopy (SSIM) (Gustafsson, 2005), stochastic optical reconstruction microscopy (STORM) (Rust and others, 2006) and (fluorescence) photoactivated localization microscopy (PALM and fPALM) (Betzig and others, 2006; Hess and others, 2006). These "nanoscopy" methods are starting to enable near molecular-scale spatial resolution in biological imaging. This review focuses on super-resolution methods based on stochastic single molecule detection and localization, such as STORM, PALM and others, with a particular focus on STORM imaging. For an overview of super-resolution methods that rely on

patterned illumination and sequential detection such as SSIM and STED the reader is directed to other reviews that include these topics (Hell, 2007; Huang and others, 2009).

General Concepts

Due to the diffraction of light, the image of a single molecule captured through a conventional optical microscope is much larger than the molecule itself (and is often referred to as point spread function or PSF). When the molecule is isolated, it is possible to determine its position with very high precision by finding the centroid of its PSF (Figure 1a) (Thompson and others, 2002; Yildiz and others, 2004). Although the ability to precisely localize single molecules is by itself powerful, this concept alone is not enough to break the diffraction limit when imaging densely-labeled samples. The resolving power of an optical microscope is related to the ability to discriminate two single molecules in close proximity and this ability is still limited by diffraction, since the PSF of these molecules will overlap when they are closer than the diffraction limit ($\lambda/2NA$). Therefore, to extend single molecule localization concept to super-resolution imaging, it is necessary to be able to actively control the density of molecules that are fluorescent at any given time to avoid overlapping images. This active control of fluorophore density was made possible by the discovery of photoswitchable probes (Bates and others, 2005; Heilemann and others, 2005; Patterson and Lippincott-Schwartz, 2002). Photoswitchable probes can be cycled between bright and dark states (or between two different spectral colors) using light illumination. In particular, the majority of probes can be "switched off" to allow only a very small fraction of them to be in the fluorescent state. Even in a densely-labeled sample, the images of this sparse subset of activated probes will no longer overlap and therefore their positions can be localized with high precision. Through iterative cycles of activation and de-activation, the positions of all the probes can be precisely determined, and these positions can then be used to reconstruct a high resolution image of the underlying structure (Figure 1b).

The spatial resolution in super-resolution microscopy depends on several factors. First, the precision by which each molecule can be localized, known as "localization precision", affects the spatial resolution. The localization precision mainly depends on the number of photons emitted by the molecule, background noise, and pixel size (Mortensen and others, 2010; Stallinga and Rieger, 2012; Thompson and others, 2002). In 2012, S. Stallinga and B. Rieger proposed an analytical expression for the localization precision (Stallinga and Rieger, 2012):

$$\sigma^2_{Localization\,Precision} = \frac{s^2 + a^2/12}{N}\left(1 + 4\tau + \sqrt{\frac{2\tau}{1+4\tau}}\right), \quad (1)$$

where s is the width of the Gaussian that is used to fit the PSF, a the pixel size, N the number of collected photons, and τ a normalized dimensionless background parameter defined as $\tau = 2\pi b\left(s^2 + a^2/12\right)/\left(Na^2\right)$, with b being the number of background photons per pixel. In practice, the localization precision can be experimentally determined by measuring the standard deviation of a cluster of multiple localizations originating from a single fluorophore (Figure 2a) (Huang and others, 2008; Rust and others, 2006).

Second, spatial resolution depends on the labeling density. Low labeling densities typically cause continuous structures to appear discontinuous, resulting in a loss of detail (Figure 2b). The effects of the labeling density on the spatial resolution can be quantified by the Nyquist criterion (Dempsey and others, 2011; Shroff and others, 2008), which states that structural features smaller than twice the fluorophore-to-fluorophore distance cannot be reliably discerned:

$$\sigma_{Nyquist} = 2/\rho^{1/D} \quad (2)$$

where ρ is the labeling density calculated as the number of localizations per unit area or volume and D is the dimension of the structure to be imaged (2 for two-dimensional and 3 for three-dimensional imaging). Methods have been developed that take into account both localization precision and labeling density to calculate the intrinsic image resolution (Nieuwenhuizen and others, 2013).

Finally, the physical size of the probe also has an effect on how accurately the final super-resolution image resembles the actual structure. Therefore, small probes such as fluorescent proteins, Fab fragments, or nanobodies (Ries and others, 2012) are highly desirable since they will more precisely report the actual position of the target molecule (Figure 2c).

Photoswitchable probes

Photoswitchable probes are at the heart of super-resolution methods that rely on single molecule detection and localization. Initially, STORM was demonstrated with the use of a fluorophore pair (Cy3-Cy5) as an optical switch (Bates and others, 2005), while PALM and fPALM were demonstrated with the use of photoactivatable green fluorescent protein (PA-GFP) (Patterson and Lippincott-Schwartz, 2002), but since then these methods have been extended to utilize a large number of other photoswitchable probes (Dempsey and others, 2011; Fernandez-Suarez and Ting, 2008; Lippincott-Schwartz and Patterson, 2009).

The paired fluorophores used in STORM are often referred to as the activator-reporter pair. In the case of Cy3-Cy5, Cy3 is the activator dye and Cy5 is the reporter dye. The reporter is typically imaged using a far-red laser until it switches to a dark state. Once in the dark state, the fluorescence of the reporter can be recovered using illumination light that matches the excitation wavelength of the activator (e.g. green light for Cy3). For this concept to work, the activator and the reporter must be in close proximity (1-2 nm)(Bates and others, 2005). A wide range of activator-reporter dyes have been shown to have similar optical switching properties as the original Cy3-Cy5 pair (Bates and others, 2012; Bates and others, 2007). In addition, small organic fluorophores have been shown to undergo photoswitching without the need for an "activator" dye (dSTORM) (Dempsey and others, 2011; Heilemann and others, 2009; Heilemann and others, 2008; van de Linde and others, 2009). In all cases, the photoswitching seems to critically depend on the buffer conditions. Typically, imaging buffers that induce photoswitching in small organic fluorophores contain reducing agents such as thiols (e.g. β-mercaptoethanol, cysteamine) (Dempsey and others, 2011; Heilemann and others, 2009), ascorbic acid (Benke and Manley, 2012), or phosphine (Vaughan and others, 2013) along with an oxygen scavenger system to remove oxygen (Dempsey and others, 2011). While some fluorophores undergo efficient photoswitching in common buffers, typically the buffer must be

optimized for each fluorophore to achieve a high photon output while minimizing the fraction of time that the fluorophore spends in the on state (known as "low duty cycle") (Dempsey and others, 2011; Olivier and others, 2013).

In addition to small organic fluorophores, a wide range of photoactivatable, photoconvertible, and photoswitchable fluorescent proteins have been developed for PALM/fPALM imaging (Lippincott-Schwartz and Patterson, 2009). Fluorescent proteins have the advantage that they are genetically encoded and therefore easier to use for intracellular labeling and live-cell imaging. However, the photon output of fluorescent proteins tends to be lower than that of small organic fluorophores, leading to inferior localization precision. Small organic fluorophores can be linked to the target structure through antibodies, Fab fragments, or nanobodies (Ries and others, 2012). For intracellular labeling in living cells, hybrid systems that combine a genetically encoded tag such as SNAP-, CLIP- or Halo-tag (Jones and others, 2011; Klein and others, 2011; Lee and others, 2010; van de Linde and others, 2012) together with a fluorophore-labeled synthetic component can be used. It is also possible to directly label certain structures, such as lipid membranes and DNA using lipophilic (Shim and others, 2012) or DNA-binding dyes (Benke and Manley, 2012; Flors, 2010), respectively. Finally, click chemistry, in which a modified target containing a terminal alkyne group reacts with a modified fluorophore containing an azide group, can be used to label proteins or nucleic acids (Zessin and others, 2012).

On the whole, the key feature to all probes for single molecule localization microscopy is their ability to toggle between different fluorescent states, making it possible to image only sparse fluorophores even in a densely labeled biological sample. Photon output, duty cycle and labeling strategies are important considerations to take into account when choosing the right probe for a specific biological application.

Multi-color super-resolution imaging

Multi-color imaging is an important capability of fluorescence microscopy. In many biological systems, it is important to visualize many different proteins or cellular components to study their interactions. The activator-reporter fluorophore pairs provide a large palette of distinguishable photoswitchable probes for multi-color STORM imaging (Bates and others, 2012; Bates and others, 2007). In this case, the number of colors that can be achieved depends on the number of distinct activator-reporter dye pairs. To date, six such pairs have been demonstrated by combinatorially pairing three distinct activator and two distinct reporter dyes (Bates and others, 2012). In biological samples, three-color imaging has been shown using three different activators paired with the same reporter (Lakadamyali and others, 2012). Using the same reporter dye while varying only the activator dye is advantageous in that image alignment of different chromatic channels does not need to be performed, since the different channels are acquired using the same fluorophore through the same optical path. While this type of imaging can be prone to color cross-talk (faulty color-assignment of those fluorophores that are spontaneously activated independently of the activation laser or falsely activated by the wrong activation laser (Bates and others, 2012; Dani and others, 2010; Lakadamyali and others, 2012)), the cross-talk can often be corrected during post-processing using statistical approaches (Dani and others, 2010). On the other hand, when using different reporter dyes for multi-color imaging (or different photoswitchable fluorophores in the absence of

an activator dye), image alignment is needed to precisely register the images acquired through the different optical paths (Annibale and others, 2012; Bates and others, 2012). In addition, different reporters or photoswitchable fluorophores may require different buffer conditions for optimal photoswitching, making it more challenging to find sets of fluorophores that are compatible with each other. Since fluorescent proteins do not require specific buffers for photoactivation, they have been successfully used for multicolor PALM/fPALM imaging (Shroff and others, 2007). However, often only a subset of these fluorescent proteins may be successfully photoactivated and therefore it is important to optimize the fluorescent protein pairs used to avoid artificially low co-localization in multi-color images (Annibale and others, 2012). Finally, hybrid approaches that combine small organic fluorophores and fluorescent proteins have also been demonstrated (Endesfelder and others, 2011).

Overall, with careful consideration of appropriate probes, color cross-talk and image registration, multi-color super-resolution imaging can be successfully realized using a variety of different strategies (Muranyi and others, 2013; van den Dries and others, 2013; Xu and others, 2013).

3D super-resolution imaging

Most biological structures are three-dimensional. A typical way to extend STORM imaging to the third dimension consists of utilizing an astigmatic lens placed between the objective and the camera in the imaging path (Huang and others, 2008). This method can yield an axial resolution of ~50 nm over a range of ~800 nm (~400 nm above and below the focal plane) (Huang and others, 2008). Due to astigmatism, molecules that are exactly in the focal plane will appear circular; those above and below the focal plane will appear elongated either horizontally or vertically (Figure 3a). With proper calibration, the ellipticity of each molecule can be converted into the molecule's z-position (Figure 3b and c). It is also possible to combine astigmatism with a dual-objective geometry in order to capture more photons and improve the z-resolution to about ~20 nm – however, at the expense of imaging depth (Xu and others, 2012).

The imaging depth of 3D super-resolution microscopy has further been extended to thick samples by combining the astigmatism approach with selective plane illumination microscopy (SPIM) (Cella Zanacchi and others, 2013; Cella Zanacchi and others, 2011). In SPIM, the sample is illuminated by a thin sheet of light along an optical path that is orthogonal to the detection axis to achieve optical sectioning (Huisken and others, 2004). A 3D image of the sample can be generated by rotating the sample. Using this approach in combination with single molecule detection and localization (individual molecule localization-selective plane illumination microscopy, IML-SPIM) Zanacchi et al. achieved a spatial resolution of <60 nm up to 50-100 µm deep inside spheroids (Cella Zanacchi and others, 2011). In addition, by using two-photon photoactivation in selective plane illumination geometry, they could further improve the image quality by reducing the scattering effects caused when imaging thick samples (Cella Zanacchi and others, 2013).

Other methods also exist for extending STORM/PALM/fPALM to three dimensions. Astigmatism belongs to a subset of methods referred to as PSF engineering. Instead of engineering the PSF to be elliptical, it is also possible to engineer other PSF types, such as a double helix (Pavani and others,

2009). In this case, the pitch of the double helix is governed by the distance from the focal plane, therefore reporting the molecule's axial position. Finally, an interferometric method, in which photons from a single molecule collected through two opposing objectives are allowed to interfere (iPALM), has also been used for 3D PALM imaging, providing an impressive axial resolution of ~10 nm (Shtengel and others, 2009).

Live-cell super-resolution imaging

One of the greatest advantages of fluorescence microscopy is the ability to image dynamic processes inside living cells in a non-invasive manner. Live-cell imaging requires the acquisition speed to be faster than the dynamics of the biological process to be studied. For STORM/PALM/fPALM, the temporal resolution is limited by the time that it takes to acquire enough localizations to satisfy the Nyquist criterion for a given spatial resolution (Huang and others, 2010; Shroff and others, 2008). This in turn can be limited by the time it takes for a fluorophore to undergo a photoswitching cycle. The photoswitching rate of small organic fluorophores can typically be increased by increasing the excitation laser power, without compromising the photon output (Jones and others, 2011). In this case it is also important to match the camera frame rate to the fluorophore photoswitching rate. Fast frame rates can typically be obtained using a smaller field-of-view (Jones and others, 2011). High temporal resolution can thus be achieved at the expense of either the spatial resolution (acquiring less localizations), the size of the field-of-view, or both. Wombacher et al. initially demonstrated live-cell dSTORM imaging of histone H2B dynamics with 20 nm spatial resolution and 10 seconds temporal resolution (Wombacher and others, 2010). Jones et al. expanded live-cell STORM imaging to 3D and multicolor, by imaging transferrin internalization through clathrin coated pits with a few second temporal and 20-30 nm spatial resolution using an EMCCD camera imaging at a frame rate of 500 Hz (Jones and others, 2011). Faster imaging with EMCCDs would result in images with very small fields-of-view. This limitation can potentially be overcome with the use of scientific complementary metal-oxide semiconductor (sCMOS) cameras that combine the advantages of high frame rates with a large field-of-view (Huang and others, 2013).

Further improvement in the temporal resolution can be achieved with recent advances in data analysis methods for localization microscopy. As previously mentioned, in order to localize molecules with high precision, their PSFs need to be non-overlapping. However, using data analysis methods such as multi-emitter fitting or sparse-signal recovery, this requirement can be relaxed, allowing also the positions of highly-overlapping PSFs to be precisely determined (Babcock and others, 2012; Cox and others, 2012; Holden and others, 2011; Zhu and others, 2012). With these approaches, image acquisition can be sped up since the Nyquist criterion can be satisfied more rapidly by activating several overlapping molecules simultaneously in each frame. Combining the advantages of multi-emitter fitting algorithms and the sCMOS camera technology, Huang et al. imaged transferrin dynamics with millisecond temporal resolution (30 reconstructed images per second) using a frame rate of 1600 Hz and a field-of-view of 13 X 13 μm^2 (Huang and others, 2013).

Another important consideration for live-cell imaging is the suitability of the probe for labeling intracellular structures in living cells. Fluorescent proteins outperform small organic fluorophores in this respect. However, since fluorescent proteins have lower photon outputs and

slower switching rates, this improvement comes at the expense of both spatial and temporal resolution.

Overall, live cell super-resolution imaging has been demonstrated using a wide range of probes and imaging conditions leading to varying levels of spatiotemporal resolution. Several parameters such as imaging speed, imaging length, spatial resolution, field-of-view and phototoxicity must be carefully considered and balanced to achieve the desired results. For a recent, more in depth review on the topic the reader is directed to (Lakadamyali, 2013).

Some recent biological applications

STORM/PALM/fPALM imaging has already led to a number of salient discoveries in biology across a large number of fields. It is beyond the scope of this review to summarize the large number of important biological discoveries. Instead, we highlight here some of the latest applications of STORM imaging.

One of the fields in which STORM imaging has made a major impact has been neuroscience. As a recent example, using multi-color, 3D STORM imaging, Xu et al. has shed important light on the organization of the actin cytoskeleton in neuronal axons and dendrites (Xu and others, 2013). In this elegant study, they discovered that in neuronal axons actin shows highly-organized, periodic, ring-like structures wrapped around the axon circumference. Spectrin, a cytoskeletal scaffolding protein, also forms ring-like structures, which alternates with the actin rings in a regular pattern. The spacing between the actin and spectrin rings is consistent with the length of a spectrin tetramer. These observations led to the conclusion that spectrin tetramers are aligned longitudinally along the axon shaft connecting adjacent actin rings together. This unique cytoskeletal arrangement seems to dictate the periodic distribution of sodium channels on the axonal membrane and may play an important role in action potential propagation.

Taking advantage of a wealth of methods ranging from 3D STORM and PALM imaging to single step photobleaching of cultured neurons and tissue slices, Specht et al. characterized the ultrastructure and the stoichiometry of receptors and scaffolding proteins at inhibitory synapses (Specht and others, 2013). In particular, they resolved the nanoscale arrangement of GABA receptor and gephryin and then measured the relative stoichiometry of these molecules. They found a one to one correspondence between GABA and gephyrin, indicating that gephyrin forms a two-dimensional scaffold in which all gephyrin molecules can contribute to receptor binding, an important finding given that the strength of neurotransmission is governed by the number of neurotransmitter receptors. This work demonstrates that the combination of super-resolution and quantitative imaging can be used to characterize molecular interactions and synaptic plasticity at the nanometer scale.

In another hybrid approach, Balint et al. combined single particle tracking with STORM imaging in a correlative and sequential way to study the impact of the microtubule cytoskeleton on motor-protein mediated cargo transport at high temporal and spatial resolution (Balint and others, 2013). By mapping the trajectories of lysosomes to the individual microtubule tracks on which these lysosomes moved, they investigated how microtubule intersections affect the motion of cargos.

They found that if the axial separation between microtubules at the intersection is sufficiently large, then cargos can pass through the intersection and continue moving on the same microtubule. However, if the microtubule separation is too small (<100 nm), cargos are forced to pause. This correlative-imaging approach is well-suited for studying how road-blocks impact cargo transport and will be useful for putting other fast cellular dynamics into the context of ultrastructure.

As a final example, Szymborska et al. very elegantly combined STORM imaging with single particle averaging to determine the molecular architecture of one of the protein complexes making up the nuclear pore complex (NPC) (Szymborska and others, 2013). They obtained super-resolution images of thousands of NPC rings by labeling the different proteins of the Nup107-160 subcomplex, one of the largest building blocks of the NPC. While the spatial resolution of each NPC ring was limited to 15-20 nm, they took advantage of the symmetry of this structure to align and average thousands of NPC images. This particle averaging approach (Loschberger and others, 2012) allowed them to resolve the position of each protein within the Nup107-160 subcomplex with 1 nm spatial resolution. As a result, they could build a model for the structural organization of the NPC scaffold. This exciting study opens the door for using super-resolution microscopy methods such as STORM to address important questions in structural biology related to the organization of large protein complexes.

Conclusions and Outlook

Since their first demonstration in 2006, single molecule localization methods such as STORM/PALM/fPALM have undergone tremendous technological developments. Nanoscopic imaging has since been extended to multiple colors, three dimensions, and living cells. In addition, rapid commercialization has made these methods more easily available to non-specialists. These advances led to a fast pace of important new discoveries in biology. Based on this early progress, it is clear that the future of super-resolution imaging holds great promise. In particular, further developments in the field of photoswitchable probes will enable exciting, new possibilities. Improvements in brightness, photostability, and photoswitching rates of available probes and the discovery of new probes with improved properties should permit long-term visualization of ultrastructural dynamics with very high spatiotemporal resolution. In addition, continued developments in three-dimensional imaging of thick samples will create new opportunities to study biological processes inside tissues (*ex vivo*) or in small animals (*in vivo*) with unprecedented spatial resolution.

Acknowledgments: This work was supported in part by Fundació Cellex, Barcelona, Marie-Curie International Reintegration Grant FP7-PEOPLE-2010-RG, and the Plan Nacional Grant from the Spanish Ministry (Ministerio de Economia y Competitividad) FIS2012-37753. Authors declare no conflict of interest.

Figures

Figure 1 – (A) The image of a single fluorophore in a light microscope is a diffraction-limited spot. By fitting a Gaussian to its intensity profile it is possible to retrieve the original position of the fluorophore with nanometer precision. (B) Schematic showing the general strategy for single molecule localization microscopy. By using photoswitchable fluorophores, it is possible to turn "on" and image only a few molecules at a time (shown in light green). These sparse, single fluorescent molecules are localized with very high precision (localizations are shown as dark green spots), turned "off" (by photobleaching or by switching to a dark state), and a new subset is turned "on". This process is repeated for several cycles until all fluorophores are localized. Finally a super-resolution image of the underlying structure can be reconstructed by adding all the localizations (last panel).

Figure 2 – (A) The localization precision in (*x*-*y*) directions can be determined from the standard deviation (σ) of the distribution of multiple localizations originating from an individual fluorophore (shown in the figure is the full width at half maximum, FWHM=2.35σ). (B) Effect of the labeling density on the spatial resolution, illustrated for the particular case of microtubules. In the zoomed-in view, a significant improvement in resolution can be appreciated as the labeling density increases. (C) Schematic comparison of the size of different types of probes: conventional antibodies (~10-15 nm), Fab fragments (~5-6 nm), and nanobodies (~4 nm).

Figure 3 – Three-dimensional STORM imaging with an astigmatic lens. (A) A molecule in the focal plane appears circular (center), while molecules above and below the focal plane appear elongated (top and bottom, respectively). (B) The position of each molecule relative to the focal plane (z=0) can be determined from a calibration plot by measuring the width of each molecule in (*x*-*y*) (Wx and Wy). (C) Example of microtubules imaged in three dimensions using this approach. The color coding indicates z-height according to the color scale bar.

References

Annibale P, Scarselli M, Greco M, Radenovic A. 2012. Identification of the factors affecting co-localization precision for quantitative multicolor localization microscopy. Optical Nanoscopy 1:9.

Babcock H, Yaron MS, Zhuang X. 2012. A high-density 3D localization algorithm for stochastic optical reconstruction microscopy. Optical Nanoscopy 1: 6.

Balint S, Verdeny Vilanova I, Sandoval Alvarez A, Lakadamyali M. 2013. Correlative live-cell and superresolution microscopy reveals cargo transport dynamics at microtubule intersections. Proc Natl Acad Sci U S A 110(9): 3375-80.

Bates M, Blosser TR, Zhuang X. 2005. Short-range spectroscopic ruler based on a single-molecule optical switch. Phys Rev Lett 94(10): 108101.

Bates M, Dempsey GT, Chen KH, Zhuang X. 2012. Multicolor super-resolution fluorescence imaging via multi-parameter fluorophore detection. Chemphyschem 13(1): 99-107.

Bates M, Huang B, Dempsey GT, Zhuang X. 2007. Multicolor super-resolution imaging with photo-switchable fluorescent probes. Science 317(5845): 1749-53.

Benke A, Manley S. 2012. Live-cell dSTORM of cellular DNA based on direct DNA labeling. Chembiochem 13(2): 298-301.

Betzig E, Patterson GH, Sougrat R, Lindwasser OW, Olenych S, Bonifacino JS, Davidson MW, Lippincott-Schwartz J, Hess HF. 2006. Imaging intracellular fluorescent proteins at nanometer resolution. Science 313(5793): 1642-5.

Cella Zanacchi F, Lavagnino Z, Faretta M, Furia L, Diaspro A. 2013. Light-sheet confined super-resolution using two-photon photoactivation. PLoS One 8(7): e67667.

Cella Zanacchi F, Lavagnino Z, Perrone Donnorso M, Del Bue A, Furia L, Faretta M, Diaspro A. 2011. Live-cell 3D super-resolution imaging in thick biological samples. Nat Methods 8(12): 1047-9.

Cox S, Rosten E, Monypenny J, Jovanovic-Talisman T, Burnette DT, Lippincott-Schwartz J, Jones GE, Heintzmann R. 2012. Bayesian localization microscopy reveals nanoscale podosome dynamics. Nat Methods 9(2): 195-200.

Dani A, Huang B, Bergan J, Dulac C, Zhuang X. 2010. Superresolution imaging of chemical synapses in the brain. Neuron 68(5): 843-56.

Dempsey GT, Vaughan JC, Chen KH, Bates M, Zhuang X. 2011. Evaluation of fluorophores for optimal performance in localization-based super-resolution imaging. Nat Methods 8(12): 1027-36.

Endesfelder U, Malkusch S, Flottmann B, Mondry J, Liguzinski P, Verveer PJ, Heilemann M. 2011. Chemically induced photoswitching of fluorescent probes--a general concept for super-resolution microscopy. Molecules 16(4): 3106-18.

Fernandez-Suarez M, Ting AY. 2008. Fluorescent probes for super-resolution imaging in living cells. Nat Rev Mol Cell Biol 9(12): 929-43.

Flors C. 2010. Photoswitching of monomeric and dimeric DNA-intercalating cyanine dyes for super-resolution microscopy applications. Photochem Photobiol Sci 9(5): 643-8.

Gustafsson MG. 2005. Nonlinear structured-illumination microscopy: wide-field fluorescence imaging with theoretically unlimited resolution. Proc Natl Acad Sci U S A 102(37): 13081-6.

Heilemann M, Margeat E, Kasper R, Sauer M, Tinnefeld P. 2005. Carbocyanine dyes as efficient reversible single-molecule optical switch. J Am Chem Soc 127(11): 3801-6.

Heilemann M, van de Linde S, Mukherjee A, Sauer M. 2009. Super-resolution imaging with small organic fluorophores. Angew Chem Int Ed Engl 48(37): 6903-8.

Heilemann M, van de Linde S, Schuttpelz M, Kasper R, Seefeldt B, Mukherjee A, Tinnefeld P, Sauer M. 2008. Subdiffraction-resolution fluorescence imaging with conventional fluorescent probes. Angew Chem Int Ed Engl 47(33): 6172-6.

Hell SW. 2007. Far-field optical nanoscopy. Science 316(5828): 1153-8.

Hess ST, Girirajan TP, Mason MD. 2006. Ultra-high resolution imaging by fluorescence photoactivation localization microscopy. Biophys J 91(11): 4258-72.

Holden SJ, Uphoff S, Kapanidis AN. 2011. DAOSTORM: an algorithm for high- density super-resolution microscopy. Nat Methods 8(4): 279-80.

Huang B, Babcock H, Zhuang X. 2010. Breaking the diffraction barrier: super-resolution imaging of cells. Cell 143(7): 1047-58.

Huang B, Bates M, Zhuang X. 2009. Super-resolution fluorescence microscopy. Annu Rev Biochem 78: 993-1016.

Huang B, Wang W, Bates M, Zhuang X. 2008. Three-dimensional super-resolution imaging by stochastic optical reconstruction microscopy. Science 319(5864): 810-3.

Huang F, Hartwich TM, Rivera-Molina FE, Lin Y, Duim WC, Long JJ, Uchil PD, Myers JR, Baird MA, Mothes W, Davidson MW, Toomre D, Bewersdorf J. 2013. Video-rate nanoscopy using sCMOS camera-specific single-molecule localization algorithms. Nat Methods 10(7): 653-8.

Huisken J, Swoger J, Del Bene F, Wittbrodt J, Stelzer EH. 2004. Optical sectioning deep inside live embryos by selective plane illumination microscopy. Science 305(5686): 1007-9.

Jones SA, Shim SH, He J, Zhuang X. 2011. Fast, three-dimensional super-resolution imaging of live cells. Nat Methods 8(6): 499-508.

Klar TA, Hell SW. 1999. Subdiffraction resolution in far-field fluorescence microscopy. Opt Lett 24(14): 954-6.

Klar TA, Jakobs S, Dyba M, Egner A, Hell SW. 2000. Fluorescence microscopy with diffraction resolution barrier broken by stimulated emission. Proc Natl Acad Sci U S A 97(15): 8206-10.

Klein T, Loschberger A, Proppert S, Wolter S, van de Linde S, Sauer M. 2011. Live-cell dSTORM with SNAP-tag fusion proteins. Nat Methods 8(1): 7-9.

Lakadamyali M. 2013. Super-resolution microscopy: going live and going fast. Chemphyschem in press.

Lakadamyali M, Babcock H, Bates M, Zhuang X, Lichtman J. 2012. 3D multicolor super-resolution imaging offers improved accuracy in neuron tracing. PLoS One 7(1): e30826.

Lee HL, Lord SJ, Iwanaga S, Zhan K, Xie H, Williams JC, Wang H, Bowman GR, Goley ED, Shapiro L, Twieg RJ, Rao J, Moerner WE. 2010. Superresolution imaging of targeted proteins in fixed and living cells using photoactivatable organic fluorophores. J Am Chem Soc 132(43): 15099-101.

Lippincott-Schwartz J, Patterson GH. 2009. Photoactivatable fluorescent proteins for diffraction-limited and super-resolution imaging. Trends Cell Biol 19(11): 555-65.

Loschberger A, van de Linde S, Dabauvalle MC, Rieger B, Heilemann M, Krohne G, Sauer M. 2012. Super-resolution imaging visualizes the eightfold symmetry of gp210 proteins around the nuclear pore complex and resolves the central channel with nanometer resolution. J Cell Sci 125(Pt 3): 570-5.

Mortensen KI, Churchman LS, Spudich JA, Flyvbjerg H. 2010. Optimized localization analysis for single-molecule tracking and super-resolution microscopy. Nat Methods 7(5): 377-81.

Muranyi W, Malkusch S, Muller B, Heilemann M, Krausslich HG. 2013. Super-resolution microscopy reveals specific recruitment of HIV-1 envelope proteins to viral assembly sites dependent on the envelope C-terminal tail. PLoS Pathog 9(2): e1003198.

Nieuwenhuizen RP, Lidke KA, Bates M, Puig DL, Grunwald D, Stallinga S, Rieger B. 2013. Measuring image resolution in optical nanoscopy. Nat Methods 10(6): 557-62.

Olivier N, Keller D, Gonczy P, Manley S. 2013. Resolution doubling in 3D-STORM imaging through improved buffers. PLoS One 8(7): e69004.

Patterson GH, Lippincott-Schwartz J. 2002. A photoactivatable GFP for selective photolabeling of proteins and cells. Science 297(5588): 1873-7.

Pavani SR, Thompson MA, Biteen JS, Lord SJ, Liu N, Twieg RJ, Piestun R, Moerner WE. 2009. Three-dimensional, single-molecule fluorescence imaging beyond the diffraction limit by using a double-helix point spread function. Proc Natl Acad Sci U S A 106(9): 2995-9.

Ries J, Kaplan C, Platonova E, Eghlidi H, Ewers H. 2012. A simple, versatile method for GFP-based super-resolution microscopy via nanobodies. Nat Methods 9(6): 582-4.

Rust MJ, Bates M, Zhuang X. 2006. Sub-diffraction-limit imaging by stochastic optical reconstruction microscopy (STORM). Nat Methods 3(10): 793-5.

Shim SH, Xia C, Zhong G, Babcock HP, Vaughan JC, Huang B, Wang X, Xu C, Bi GQ, Zhuang X. 2012. Super-resolution fluorescence imaging of organelles in live cells with photoswitchable membrane probes. Proc Natl Acad Sci U S A 109(35): 13978-83.

Shroff H, Galbraith CG, Galbraith JA, Betzig E. 2008. Live-cell photoactivated localization microscopy of nanoscale adhesion dynamics. Nat Methods 5(5): 417-23.

Shroff H, Galbraith CG, Galbraith JA, White H, Gillette J, Olenych S, Davidson MW, Betzig E. 2007. Dual-color superresolution imaging of genetically expressed probes within individual adhesion complexes. Proc Natl Acad Sci U S A 104(51): 20308-13.

Shtengel G, Galbraith JA, Galbraith CG, Lippincott-Schwartz J, Gillette JM, Manley S, Sougrat R, Waterman CM, Kanchanawong P, Davidson MW, Fetter RD, Hess HF. 2009. Interferometric fluorescent super-resolution microscopy resolves 3D cellular ultrastructure. Proc Natl Acad Sci U S A 106(9): 3125-30.

Specht CG, Izeddin I, Rodriguez PC, El Beheiry M, Rostaing P, Darzacq X, Dahan M, Triller A. 2013. Quantitative nanoscopy of inhibitory synapses: counting gephyrin molecules and receptor binding sites. Neuron 79(2): 308-21.

Stallinga S, Rieger B. 2012. The effect of background on localization uncertainty in single emitter imaging. IEEE Int Symp Biomedical Imaging: 988-991.

Szymborska A, de Marco A, Daigle N, Cordes VC, Briggs JA, Ellenberg J. 2013. Nuclear pore scaffold structure analyzed by super-resolution microscopy and particle averaging. Science 341(6146): 655-8.

Thompson RE, Larson DR, Webb WW. 2002. Precise nanometer localization analysis for individual fluorescent probes. Biophys J 82(5): 2775-83.

van de Linde S, Endesfelder U, Mukherjee A, Schuttpelz M, Wiebusch G, Wolter S, Heilemann M, Sauer M. 2009. Multicolor photoswitching microscopy for subdiffraction-resolution fluorescence imaging. Photochem Photobiol Sci 8(4): 465-9.

van de Linde S, Heilemann M, Sauer M. 2012. Live-cell super-resolution imaging with synthetic fluorophores. Annu Rev Phys Chem 63: 519-40.

van den Dries K, Schwartz SL, Byars J, Meddens MB, Bolomini-Vittori M, Lidke DS, Figdor CG, Lidke KA, Cambi A. 2013. Dual-color superresolution microscopy reveals nanoscale organization of mechanosensory podosomes. Mol Biol Cell 24(13): 2112-23.

Vaughan JC, Dempsey GT, Sun E, Zhuang X. 2013. Phosphine quenching of cyanine dyes as a versatile tool for fluorescence microscopy. J Am Chem Soc 135(4): 1197-200.

Wombacher R, Heidbreder M, van de Linde S, Sheetz MP, Heilemann M, Cornish VW, Sauer M. 2010. Live-cell super-resolution imaging with trimethoprim conjugates. Nat Methods 7(9): 717-9.

Xu K, Babcock HP, Zhuang X. 2012. Dual-objective STORM reveals three-dimensional filament organization in the actin cytoskeleton. Nat Methods 9(2): 185-8.

Xu K, Zhong G, Zhuang X. 2013. Actin, spectrin, and associated proteins form a periodic cytoskeletal structure in axons. Science 339(6118): 452-6.

Yildiz A, Park H, Safer D, Yang Z, Chen LQ, Selvin PR, Sweeney HL. 2004. Myosin VI steps via a hand-over-hand mechanism with its lever arm undergoing fluctuations when attached to actin. J Biol Chem 279(36): 37223-6.

Zessin PJ, Finan K, Heilemann M. 2012. Super-resolution fluorescence imaging of chromosomal DNA. J Struct Biol 177(2): 344-8.

Zhu L, Zhang W, Elnatan D, Huang B. 2012. Faster STORM using compressed sensing. Nat Methods 9(7): 721-3.

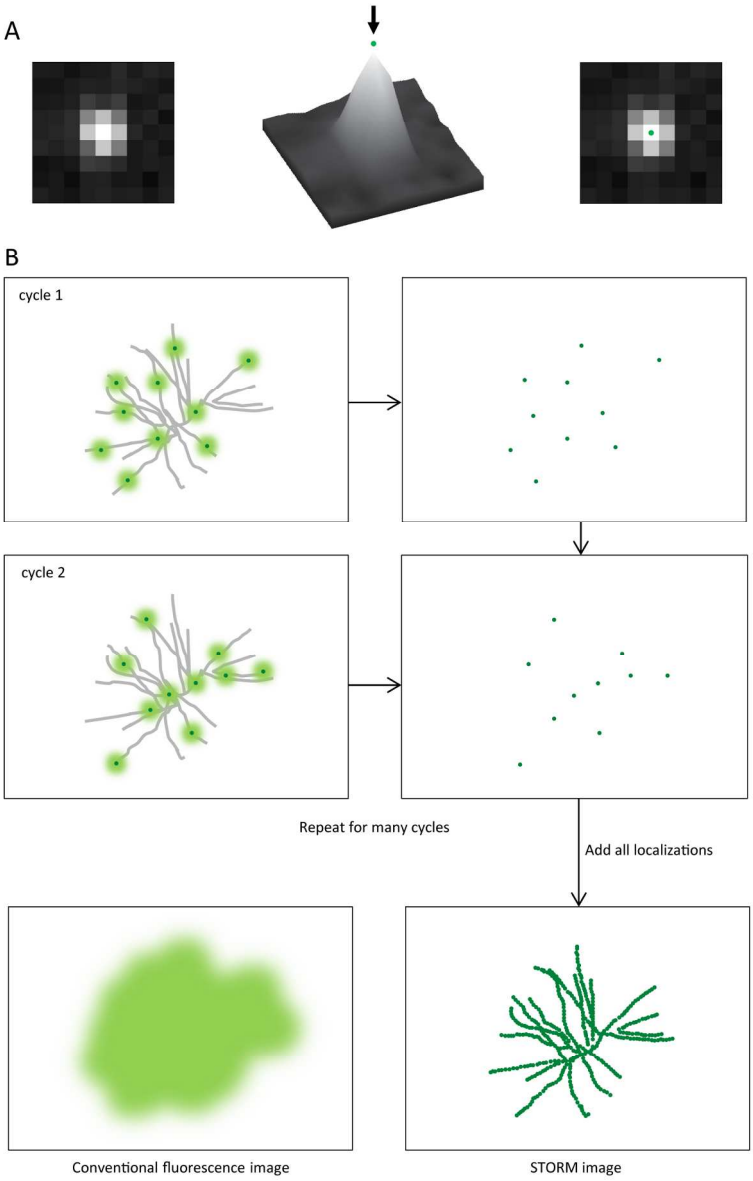

(A) The image of a single fluorophore in a light microscope is a diffraction-limited spot. By fitting a Gaussian to its intensity profile it is possible to retrieve the original position of the fluorophore with nanometer precision. (B) Schematic showing the general strategy for single molecule localization microscopy. By using photoswitchable fluorophores, it is possible to turn "on" and image only a few molecules at a time (shown in light green). These sparse, single fluorescent molecules are localized with very high precision (localizations are shown as dark green spots), turned "off" (by photobleaching or by switching to a dark state), and a new subset is turned "on". This process is repeated for several cycles until all fluorophores are localized. Finally a super-resolution image of the underlying structure can be reconstructed by adding all the localizations (last panel).
137x212mm (300 x 300 DPI)

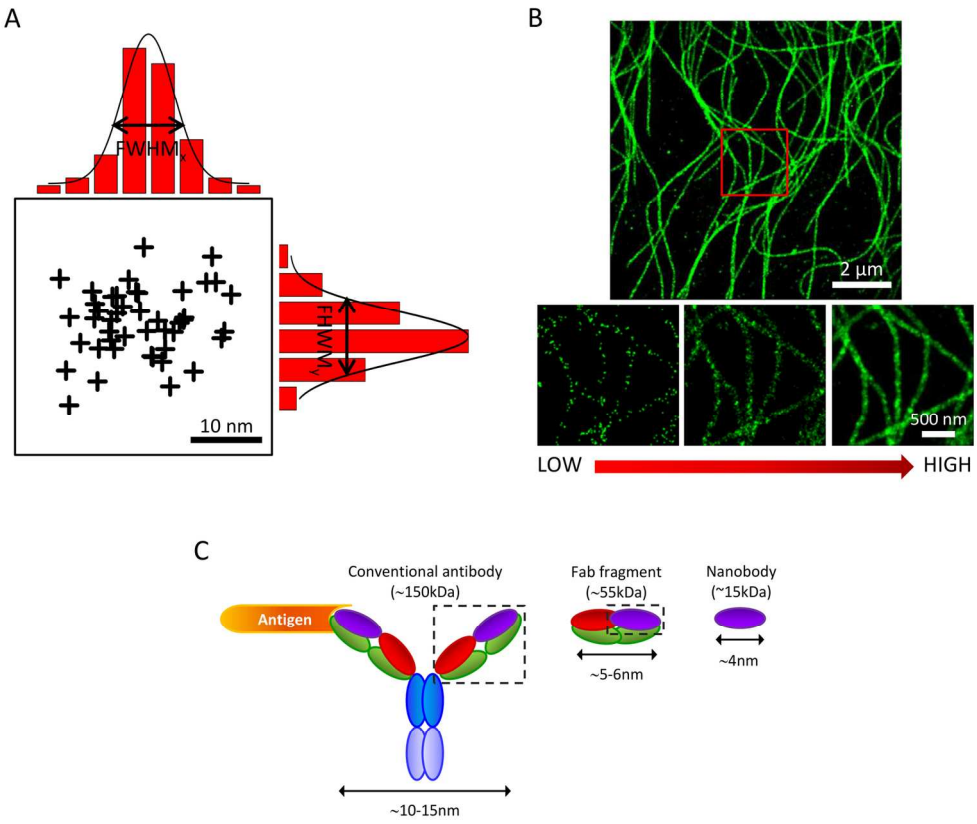

(A) The localization precision in (x-y) directions can be determined from the standard deviation (σ) of the distribution of multiple localizations originating from an individual fluorophore (shown in the figure is the full width at half maximum, FWHM=2.35σ). (B) Effect of the labeling density on the spatial resolution, illustrated for the particular case of microtubules. In the zoomed-in view, a significant improvement in resolution can be appreciated as the labeling density increases. (C) Schematic comparison of the size of different types of probes: conventional antibodies (~10-15 nm), Fab fragments (~5-6 nm), and nanobodies (~4 nm).
154x130mm (300 x 300 DPI)

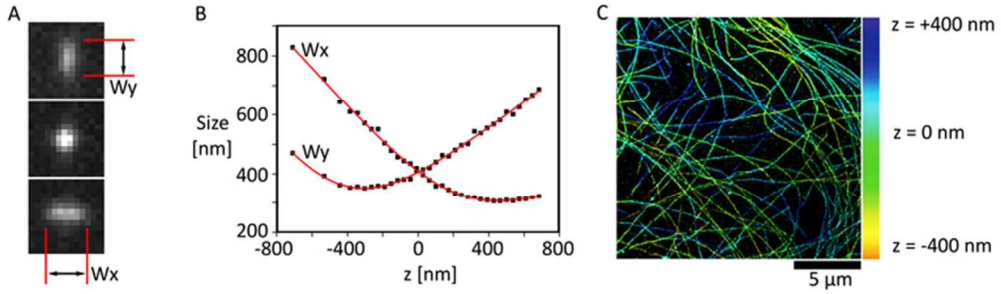

Three-dimensional STORM imaging with an astigmatic lens. (A) A molecule in the focal plane appears circular (center), while molecules above and below the focal plane appear elongated (top and bottom, respectively). (B) The position of each molecule relative to the focal plane (z=0) can be determined from a calibration plot by measuring the width of each molecule in (x-y) (Wx and Wy). (C) Example of microtubules imaged in three dimensions using this approach. The color coding indicates z-height according to the color scale bar.
64x18mm (300 x 300 DPI)